Examination of Dodd and Deeds solutions for a transmitreceive eddy current probe above a layered planar structure

Mark S. Luloff; Jordan Morelli; Thomas W. Krause

AIP Conf. Proc. 1806, 110004 (2017) https://doi.org/10.1063/1.4974682





Articles You May Be Interested In

Comparison of analytical eddy current models using principal components analysis

AIP Conf. Proc. (February 2017)

Eddy current probe characterization for model input and validation

AIP Conf. Proc. (May 2000)

Conductivity Profile Determination by Eddy Current for Shot Peened Superalloy Surfaces Toward Residual Stress Assessment

AIP Conf. Proc. (March 2007)

Examination of Dodd and Deeds Solutions for a Transmit-Receive Eddy Current Probe above a Layered Planar Structure

Mark S. Luloff ^{1,2}, Jordan Morelli ¹ and Thomas W. Krause ^{2,a}

¹Department of Physics, Engineering Physics, and Astronomy, Queen's University ²Department of Physics, Royal Military College of Canada

a) Corresponding author: Thomas.Krause@rmc.ca

Abstract. Exact solutions for the electromagnetic response of a transmit-receive coil pair situated above two parallel plates separated by a gap, were developed using the recently published general model of Desjardins *et al.* that accounts for all electromagnetic interactions between the voltage-driven probe and the conducting samples. This model was then compared to the well-known model developed by Dodd and Deeds, which assumes a constant amplitude sinusoidal current and an open-circuit pick-up coil. Both models were compared with experimental results that measured the gap profile for a Grade 2 Titanium plate (54 $\mu\Omega$ ·cm) over a SS-316 stainless steel second layer plate (74 $\mu\Omega$ ·cm). These materials simulated the electromagnetic properties of a Zr 2.5% Nb pressure tube and Zr-2 calandria tube, respectively, as found in the fuel channels of CANDU® reactors. It was observed that while the Dodd and Deeds' model as applied to this work achieved a good shape agreement with experimental data for excitation frequencies at 2 kHz, at the higher frequency of 16 kHz good agreement was not achieved. In contrast, the model of Desjardin's *et al.*, adapted for a transmit-receive probe configuration above two infinite flat plates, achieved an excellent shape agreement at both frequencies.

INTRODUCTION

In recent years, there has been a large demand for analytical models of Eddy Current (EC) probes to meet life management requirements of layered conductive structures in aging nuclear, aerospace and petrochemical infrastructure components [1, 2, 3]. The widely-used model developed by Dodd and Deeds [4, 5, 6, 7] is generally implemented as a theoretical basis for modeling EC problems [1, 2, 3]. However, Dodd and Deeds' [4, 5, 6, 7] model is only valid for open-circuit pickup coils and a constant amplitude sinusoidal drive coil current [2, 8]. For voltage-controlled systems, the constant amplitude sinusoidal drive coil current assumption is challenged as the coil currents are constantly perturbed by the feedback effects from nearby conductors. The open-circuit pickup coil assumption is also problematic because Dodd and Deeds' model cannot accurately model an experimental apparatus where the input impedance of the data acquisition system is not very large, resulting in a non-negligible current in the pickup coil.

The motivation for this paper was to compare Dodd and Deed's [4, 5, 6, 7] model with the recently published general model of Desjardins *et al.* [9, 10] for a transmit-receive eddy current probe above a dual-layered plate structure with finite coil impedances and a voltage control excitation. The model of Desjardins *et al.* [9, 10] is valid for voltage control and pickup coils with finite impedances. In addition Desjardins *et al.* 's model [9, 10] is also applicable for modeling pulsed excitations, where the feedback on the excitation coil becomes significant (this is especially true for ferromagnetic conducting materials [9, 10]).

THEORY

A transmit-receive probe typically consists of a non-coaxial drive and pickup coil pair. A time-harmonic voltage is applied to the drive coil, which generates a time-varying magnetic field and induces ECs in the nearby conducting materials [9, 10]. From Faraday's law, an electromotive force (emf) is developed in the drive and pickup coils from the changing magnetic flux arising from the drive coil source current [9, 10]. These forms of electromagnetic coupling

are mathematically described as the self-inductance L and mutual inductance M of the probe, respectively [11]. The self and mutual inductances are only dependent on the coil geometries and their relative spacing. Furthermore, the time-dependent magnetic field generated by the coils induces eddy currents in the nearby conducting structure. These ECs generate an opposing magnetic field that produces an additional emf in both coils as per Lenz's law [11]. A lossy self-inductance L is generated by the coil coupling to the ECs it generates [9, 10]. Similarly, a lossy-mutual inductance M is generated when a coil couples to the ECs generated by a neighbouring coil [9, 10]. These lossy terms are complex-valued, frequency-dependent coefficients, which may be obtained by solving the boundary conditions imposed by the conductive structure [9, 10]. As shown in Fig. 1, the assumptions required by Dodd and Deeds' model [6, 7, 5, 4] eliminate three of the six modes of electromagnetic coupling, thereby limiting the complete representation of experimental conditions. The induced voltage signal in the pickup coil $\varepsilon_p(\omega)$ can be expressed in terms of the drive coil current $I_d(\omega)$.

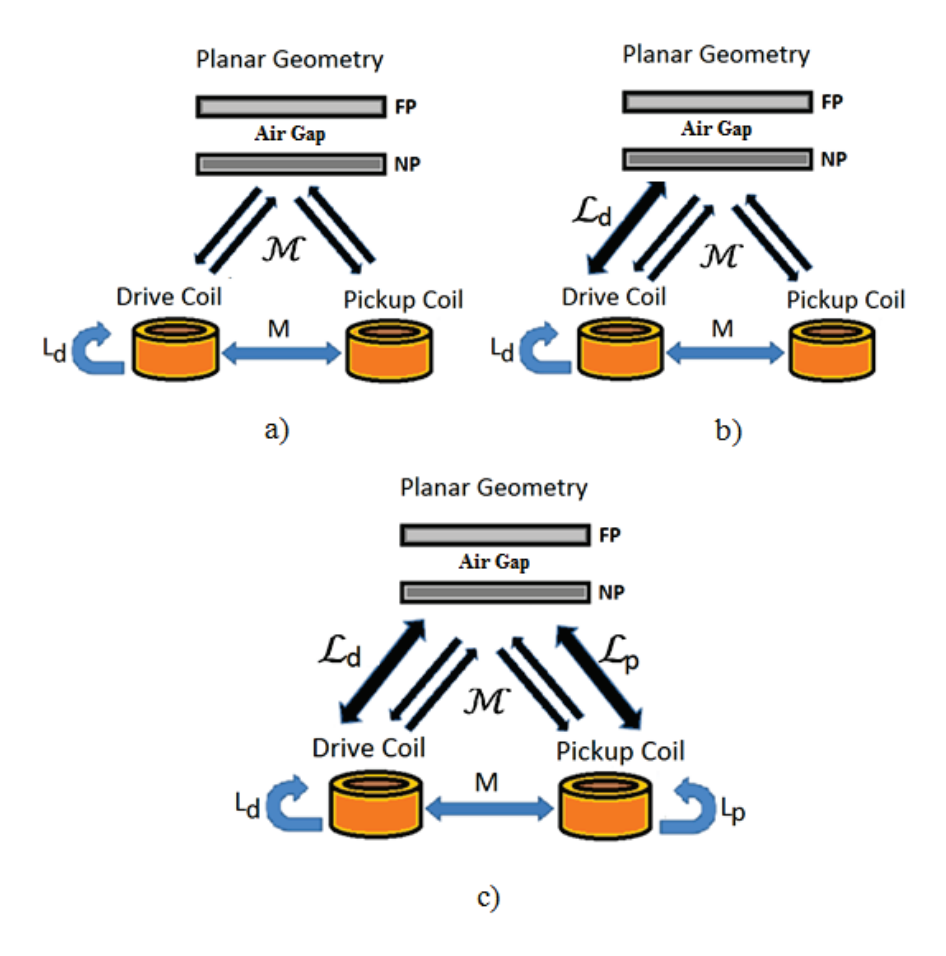


FIGURE 1. A visual presentation showing all electromagnetic interactions as addressed by (a) Dodd and Deeds' model with constant amplitude sinusoidal drive coil current approximation, (b) Dodd and Deed's model without the constant amplitude sinusoidal drive coil current approximation (or Desjardins *et al.*'s model with open-circuit pickup coils) and c) the general model of Desjardins *et al.* NP is the near plate and FP is the far plate.

An equivalent circuit model for the two-coil probe and experimental apparatus used in this work is shown below in Figure 2. For this work, a MS5800 [12] EC instrument was used as a power supply for the drive coil and as a data acquisition system for the pickup coil. The predicted signal in the pickup coil obtained from Dodd and Deeds' model with and without the Constant Amplitude Alternating Current (CAAC) approximation, and the general model of Desjardins *et al.* are shown below in Table 1.

110004-2

¹ This is equivalent to Desjardins et al.'s [12, 13] general model with open circuit pickup coils.

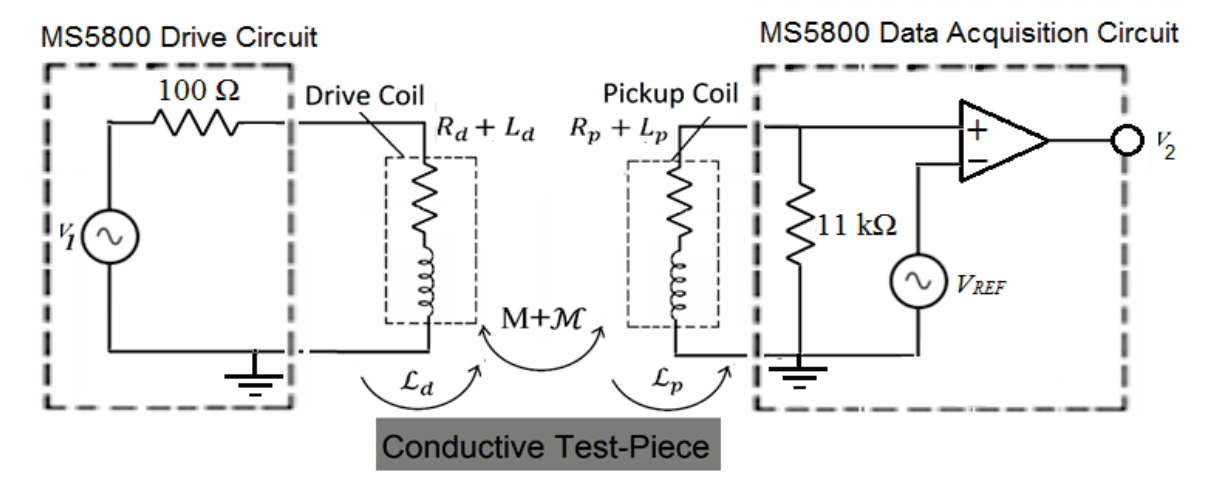


FIGURE 2. Equivalent circuit model for a driver-pickup eddy current probe. V_1 and V_2 are the power supply voltage, and the output of the data acquisition system, respectively. R, L, and L are the coil resistance, self-inductance and lossy self-inductance, respectively. The subscripts d and p denote drive and pickup coil, respectively. V_{REF} is a reference voltage to offset the data, which is chosen by the experimenter. M and M are the mutual and lossy mutual inductances between the two coils, respectively.

TABLE 1. A comparison of the three general EC models. CAAC and OC denote Constant Amplitude Alternating Current and Open Circuit, respectively.

Model	$\varepsilon_p(\omega)$	$I_d(\omega)$
Dodd and Deeds [6] with CAAC.	$j\omega(M+\mathcal{M})I_d(\omega)$	$\frac{V(\omega)}{(R'_d + j\omega L_d)}$
Dodd and Deeds [6] without CAAC	$j\omega(M+\mathcal{M})I_d(\omega)$	$\frac{V(\omega)}{\left(R'_d + j\omega(L_d + \mathcal{L}_d)\right)}$
Desjardins <i>et al</i> . [13]	$\frac{j\omega(M+\mathcal{M})}{1+\frac{j\omega(L_p+\mathcal{L}_p)}{R'_p}}I_d(\omega)$	$\frac{V(\omega)}{\left(\mathbf{R'}_d + j\omega(\mathbf{L}_d + \mathcal{L}_d)\right) + \frac{\omega^2(\mathbf{M} + \mathcal{M})^2}{\left(\mathbf{R'}_p + j\omega(\mathbf{L}_p + \mathcal{L}_p)\right)}}$

In Table 1, R'_d and R'_p are the effective resistances of the drive and pickup coil, respectively. R'_d is the sum of the drive coil resistance and the input resistance of the power supply (100 Ω) that excites the drive coil, and R'_p is the sum of the pickup coil resistance and the input resistance of the data acquisition system (11 k Ω). In many cases (generally with low-inductance pickup coils and non-ferromagnetic test pieces), Dodd and Deeds' model [6, 7, 5, 4] yields excellent agreement with experiment and has been used to successfully model a number of EC problems [14]. However, it is not widely known when the Dodd and Deeds model [6, 7, 5, 4] will be less accurate. As a first step Desjardins et al. [15] derived the following inequality, which when valid, predicts when Dodd and Deeds model (without the CAAC) [6, 7, 5, 4] will become less accurate due to the assumption of an open-circuit pickup coil.

$$\left| \frac{j\omega(L_p + \mathcal{L}_p)}{R_p} \right| \gg 1. \tag{1}$$

EXPERIMENTAL METHOD

As described in Ref. [15], the self-inductances of the probe were measured using a B&K Precision 878B LCR meter. The mutual inductance was measured by injecting a controlled AC current into the drive coil using a Keithley 6221 current source and measuring the resulting voltage in the pickup coil using an Agilent DSO-X 2012A digital oscilloscope.

An Olympus NDT Multi-scan MS5800 [12] instrument was used to perform the EC tests. This instrument was chosen because it has an internal power supply, a data acquisition system, and a user-friendly software interface to perform data manipulation and can communicate with most computers. Furthermore, the MS5800 automatically determines the phase and amplitude of the reference signal V_{REF} required to null each channel on a known calibration standard, and can perform digital filtering without the need for additional electronics. The input resistance of the data acquisition system MS5800 is finite (11 k Ω), which will test the limitations of Dodd and Deeds' model.

In order to obtain the response of the eddy current probe to a change in gap, the probe was first fixed to the NP, which was a 3.18 ± 0.01 mm thick sheet of Grade 2 Titanium ($53.9\pm0.5~\mu\Omega\cdot cm$). The probe was then nulled. The probe and near-plate were separated from a 1.20 ± 0.01 mm thick sheet of non-ferromagnetic SS-316 stainless steel ($74.5\pm0.7~\mu\Omega\cdot cm$) by up to thirteen 1.02 ± 0.05 mm thick plastic shims to create a precise air gap. Shims were progressively removed to measure the plate-gap profile (13~mm to 0~mm) for the probe.

RESULTS AND DISCUSSION

The gap profiles for the Grade 2 Titanium NP and SS-316 FP were calculated from the different analytical models and compared with experimental measurements at 1.9 kHz and 16 kHz, respectively. Figure 3 shows the predicted amplitude and phase of the 2 kHz gap profile calculated from Dodd and Deeds [6, 7, 5, 4] model with the CAAC and Desjardins *et al.*'s general model [9, 10] with and without open circuit pickup coils. Figure 4 shows the predicted amplitude and phase of the 16 kHz gap profile calculated from Dodd and Deeds model with the CAAC approximation [6, 7, 5, 4], and Desjardins *et al.*'s [9, 10] general model with and without open circuit pickup coils. Figure 5 compares the predicted 1.9 kHz and 16 kHz impedance plane displays of the gap profiles for the three different models. Figure 6 and Figure 7 compare the predicted impedance plane display of the 1.9 kHz and 16 kHz gap profile calculated from Desjardins *et al.*'s [9, 10] finite-impedance model and Dodd and Deeds [6, 7, 5, 4] solutions against experimental data.

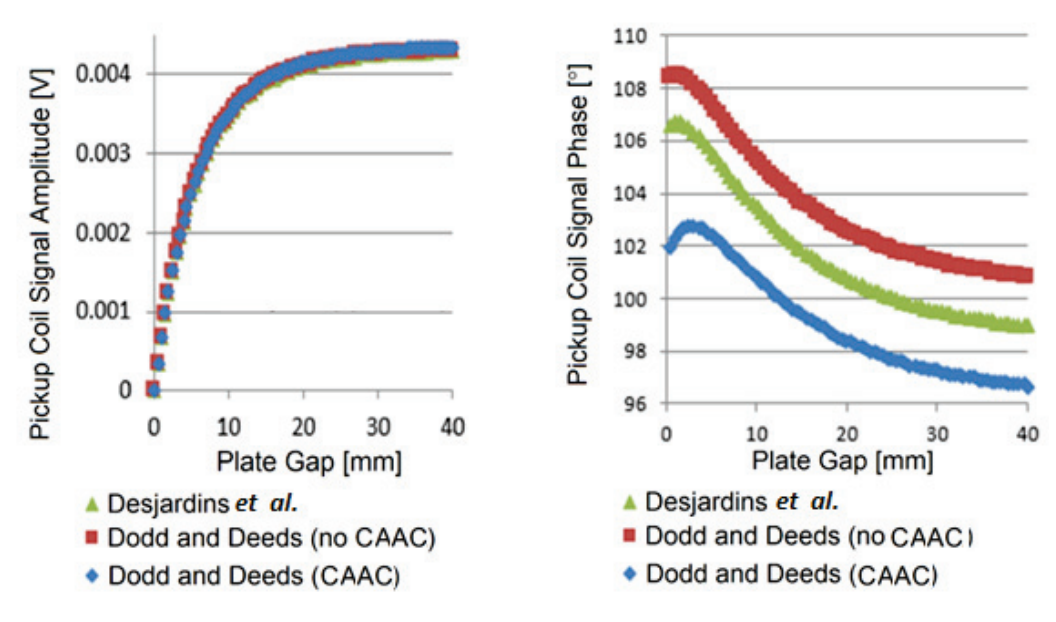


FIGURE 3. Predicted amplitude (left) and phase response (right) of the 1.9 kHz plate gap profile.

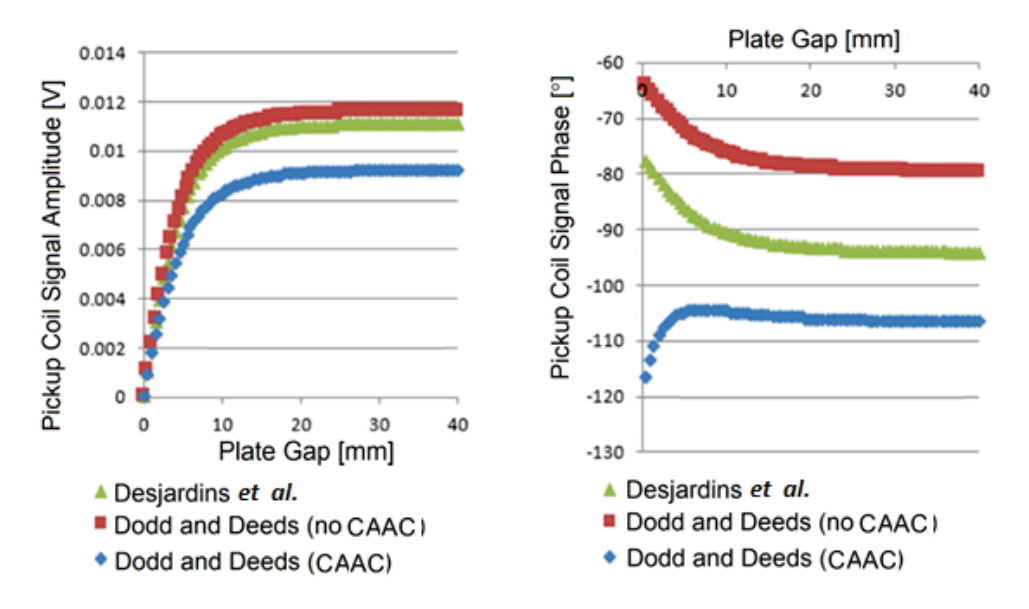


FIGURE 4. Predicted amplitude (left) and phase response (right) of the 16 kHz plate gap profile.

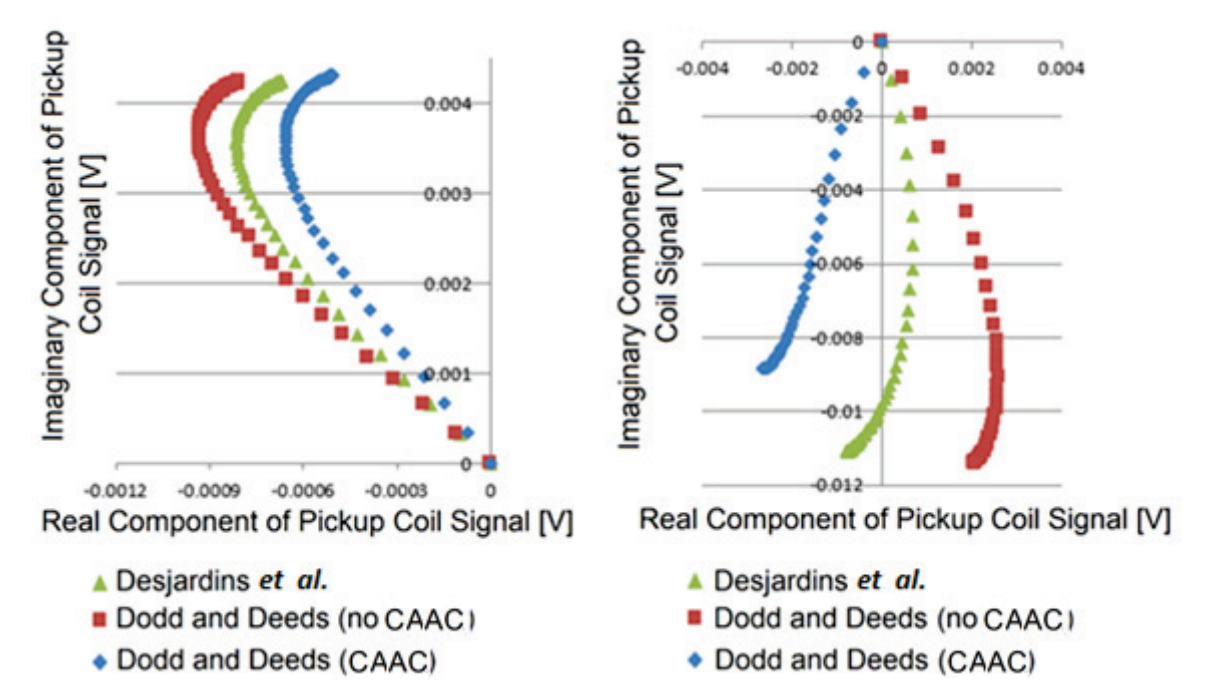


FIGURE 5. Predicted impedance plane display of the 2 kHz (left) and 16 kHz (right) plate gap profile.

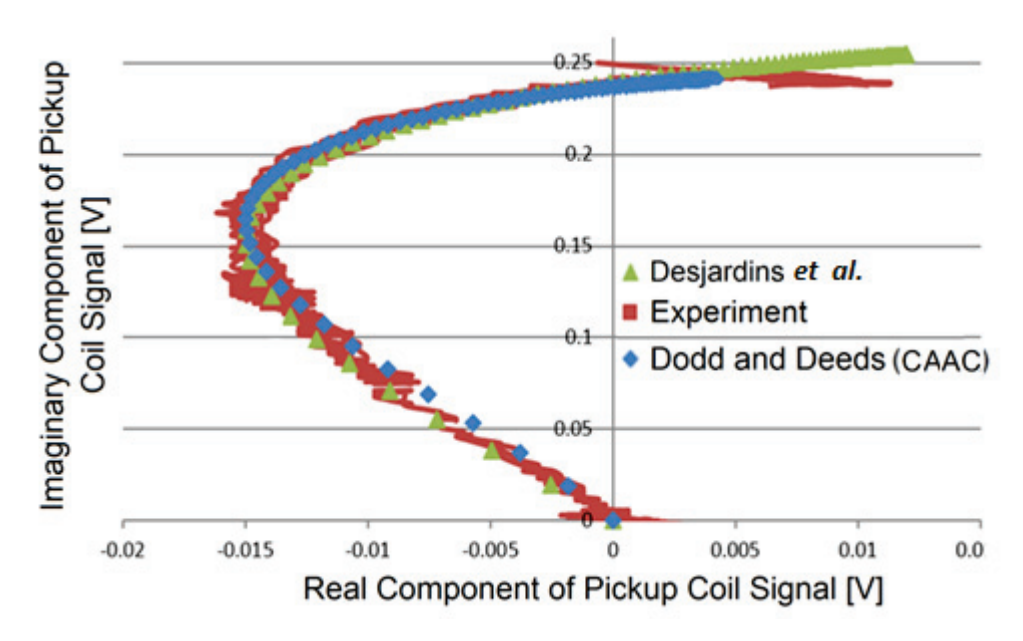


FIGURE 6. Impedance plane display comparing the analytic models and experimentally measured 1.9 kHz gap profiles. Gap increases from left to right from ~ 0 mm to 13 mm. The data was nulled at 0 mm gap and 1.9 mm liftoff. The Dodd and Deeds model without the CAAC was not plotted, because after a scaling and rotation operation, achieved a near-perfect match to the general model of Desjardins *et al*.

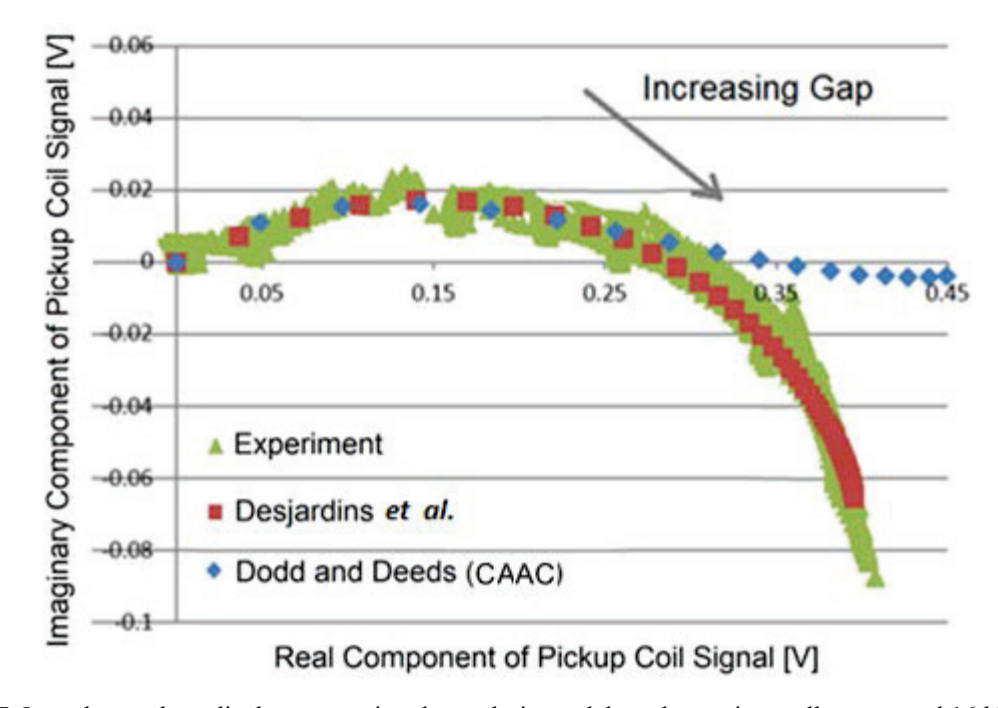


FIGURE 7. Impedance plane display comparing the analytic models and experimentally measured 16 kHz gap profiles. Gap increases from left to right from ~0 mm to 13 mm. The data was nulled at 0 mm gap and 1.9 mm liftoff The Dodd and Deeds model without the CAAC was not plotted because after a scaling and rotation operation achieved a near-perfect match to the general model of Desjardins *et al*.

As shown above in Fig. 3, at low frequencies (1.9 kHz), there is virtually no difference between the different models' prediction of the amplitude response of the gap profile. Fig. 5 confirms that the Dodd and Deeds model (with and without the CAAC) [6, 7, 5, 4] is a reasonable approximation of experimental measurements at low

frequencies. In the high frequency regime (16 kHz), there are large discrepancies between the predicted amplitude and phase responses between the three models. It was found however, that for both the 1.9 kHz and 16 kHz experimental data, the Dodd and Deeds model without the CAAC could be scaled and rotated to match the Desjardins *et al.* model without a significant loss of accuracy. For this reason, the Dodd and Deeds model without the CAAC was not plotted in Fig. 5 and Fig. 6. However, as shown in Fig. 6, Dodd and Deeds [6, 7, 5, 4] model with the CAAC cannot achieve a shape agreement with experimental data, while the general model of Desjardins *et al.* [9, 10] yields an excellent match. It would seem that because the drive coil has a small impedance (\sim 10 2 Ω), its source current is highly susceptible to its lossy self-inductance as described by Eqn. (1). In the low frequency regime, the drive coil lossy self-inductance has a negligible response and therefore, the Dodd and Deeds [6, 7, 5, 4] model with the CAAC is a reasonable approximation.

CONCLUSIONS

This paper compared Dodd and Deeds' [6, 7, 5, 4] and Desjardins *et al.*'s [9, 10] models for the application of a transmit-receive EC probe in a layered planar geometry, consisting of Grade 2 Titanium (54±1 $\mu\Omega$ ·cm), and nonferromagnetic SS-316 stainless steel (74.5±0.7 $\mu\Omega$ ·cm). It was observed that at low frequencies (~2 kHz), there was no detectable difference between the different models' prediction of amplitude response to changes in gap between the plates. However, comparison with experimental data showed that Dodd and Deeds' model as applied to this work could not achieve a good shape agreement with experimental data for excitation frequencies of 16 kHz. In contrast, the general model of Desjardins *et al.* [9, 10] yielded an excellent match with experimental data for both excitation frequencies tested. Limitations in Dodd and Deeds [6, 7, 5, 4] model, including the assumption of a constant amplitude alternating current for voltage driven probes and approximating the pickup coil as an open circuit, were considered as the factors that confounded good agreement of the model and experimental results.

ACKNOWLEDGMENTS

This work was supported by University Network of Excellence in Nuclear Engineering and the Natural Sciences and Engineering Research Council of Canada.

REFERENCES

- 1. T.L.Cung, P. Joubert, and E. Vourc'H, "Eddy Current Evaluation of Air-Gaps in Aeronautical Multi-layered Assemblies Using a Multi-Frequency Behavior Model" Measurement", Elsevier. **44**(6), 1108-1116, (2011).
- S. Shokralla, S. Sullivan, J. Morelli, and T.W. Krause, "Modelling and Validation of Eddy Current Response to Changes in Factors Affecting Pressure to Calandria Tube Gap Measurement," NDT & E International 73, 3147-3154, (2015).
- 3. R.A. Smith, D. Edgar, and J.A. Skramstad, "Advances in Transient Eddy-Current Imaging for Aerospace Applications," [Online], Available: http://www.ndt.net/article/wcndt2004/pdf/aerospace/436_smith.pdf. Accessed August 18 2016.
- 4. C.V. Dodd, "Some Eddy Current problems and their Integral Solutions. Technical report contract No. W-7505-eng-26, Oak Ridge National Laboratory; April 1969.
- 5. C.C. Cheng, C.V. Dodd, and W.E. Deeds, "General Analysis of Probe Coils Near Stratified Conductors," International Journal of Nondestructive Testing, Vol. 3, pp. 109-130, (1971).
- 6. C.V. Dodd, "Solutions to Electromagnetic Induction Problems," Ph.D. Dissertation, University of Tennessee, Knoxville, TN, (1967).
- 7. C.V. Dodd, and W.E. Deeds "Calculation of Magnetic Fields From Time-Varying Currents In the Presence of Conductors," Technical report contract No. W-7405-eng-26, Oak Ridge National Laboratory; July 1975.
- 8. S. Shokralla, J. Morelli, and T.W. Krause, "Principal Components Analysis of Multi-frequency Eddy Current Data Used to Measure Pressure Tube to Calandria Tube Gap," IEEE Sensors Journal, 16, 3147-3154, (2016).
- 9. D. Desjardins, T.W. Krause, A. Tetervak, and L. Clapham, "Concerning the Derivation of Exact Solutions to Inductive Circuit Problems for Eddy Current Testing," NDT&E International, 68, 128-135, (2014).

- 10. D. Desjardins, T. W. Krause, and L. Clapham, "Transient Response of a Driver-Pickup Coil Probe in Transient Eddy Current Testing," NDT&E International, 75, 8–14, (2015).
- 11. D.J. Griffiths, "Introduction to Electrodynamics" 3rd edition. Prentice Hall, (1999).
- 12. "MultiScan MS5800 User Manual," Olympus, 27-50 (2003).
- 13. D. Desjardins, "Analytical Modelling for a Transient Probe Response in Eddy Current Testing," Ph.D. dissertation, Physics Dept, Queen's University, Kingston, Ontario, Canada (2015).
- 14. S. Sullivan, "Mathematical Modeling of X-Probe Eddy Current Array Coils Used in Tube Inspection," CNDE Journal, 6-11, Nov/Dec, (2004).
- 15. "M.S. Luloff, J. Morelli and T. W. Krause, "Solution for a Transmit-Receive Eddy Current Probe above a Layered Planar Conductive Structure." *NDT&E International (to be published)* (2016).